Resesarch Article

iMedPub Journals
http://www.imedpub.com/

Journal of Biomedical Sciences
ISSN 2254-609X

2018
Vol.7 No.3:8

DOI: 10.4172/2254-609X.100087

Spectroscopic Investigation of Procaine Interaction with Human Serum Albumin

Husain Alsamamra[1*] , Imtiaz Khalid[2], Rania Alfaqeh[1], Maryiam Farroun[3], Musa Abuteir[1] and Saqer Darwish[1]

[1]Physics Department, Al-Quds University, Palestine

[2]Chemstry Department, Birzeit University, Palestine

[3]Nano Technology Center, Al-Quds University, Palestine

[*]**Corresponding author:** Husain Alsamamra, Physics Department, Al-Quds University, Palestine, Tel: 00972-5297166009; E-mail: hsamamra@staff.alquds.edu

Received date: May 15, 2018; **Accepted date:** July 2, 2018; **Published date:** July 5, 2018

Citation: Alsamamra H, Khalid I, Alfaqeh R, Farroun M, Abuteir M, et al. (2018) Spectroscopic investigation of Procaine Interaction with Human Serum Albumin. J Biomedical Sci Vol.7 No.3:8.

Abstract

The interaction of Human Serum Albumin (HSA) with local anaesthetic, procaine hydrochloride is an important study from the viewpoint of pharmaceutical sciences to clarify the structure, function, and properties of HSA-drug complexes.

The investigation has been carried through UV-absorption, Fluorescence and FTIR spectroscopy. The secondary structure of the protein and the binding mechanisms of the drug have been studied using Fourier self-deconvolution techniques on the obtained IR spectra.

Analysis of UV-absorbance and fluorescence spectra of procaine-HSA complexes showed a weak binding ability in quenching the intrinsic fluorescence of HSA by combinations of static and dynamic quenching procedures.

The binding constant (k) is calculated by graphical analysis and found to be in the range of (1.115-1.156) × 103 M^{-1} at 293 K. Spectral analysis of HSA-procaine compound has revealed a relative decrease in the intensity of the absorption band of α helix relative to that of β-sheets. This change in intensity is mainly due to the formation of H-bonding in procaine-HSA complex.

Keywords: Procaine; HSA; Binding constant; Protein secondary structure; FT-IR spectroscopy

Introduction

Procaine hydrochloride, 2-(diethyl amino) ethyl p-amino benzoate has the molecular, formula C13H21 ClN2 O2.HCl, and its chemical structure is shown in **Figure 1** [1]. It is a local anesthetic drug applied as an injection during surgery or other medical and dental procedures. It functions as a sodium channel blocker to ease the pain and it is known to be a short acting intravenous drug with adverse side effects such as cardiac and neurological toxicity [2]. Other studies on procaine have shown it to increase dopamine and serotonin in the brains of animals [3].

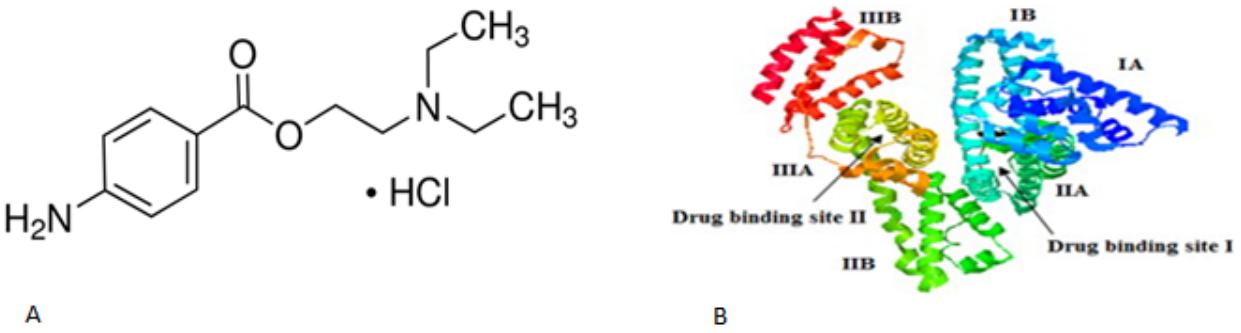

Figure 1: (A) Is the chemical structure of procaine (B) is the chemical structure of HSA.

Human serum albumin (HSA) is composed of three homologous domains (I - III): I (residues 1-195), II (residues (196-383) and III (residues 384-585) and each of which is divided into two subdomains (A and B) and able to bind to a large

number of ligands at two main binding sites, identified as site I and site II which are shown in **Figure 1B** [4-6]. Site I is dominated by strong hydrophobic interaction with most neutral, bulky, heterocyclic compounds, while site II is dominated by dipole-dipole, van der Waals, and/or hydrogen-bonding interactions - with many aromatic carboxylic acids [7].

HSA is a single monomeric protein formed by 585 amino acids with 0.6 mM concentration in the blood plasma [8]. HSA has a dominant role in transporting and arranging various compounds such as fatty acids, hormones, tryptophan, steroids, metal ions, therapeutic agents and large number of drugs. HSA is considered as the major solvable protein components of the circulatory system, contributing to colloidal oncotic blood its pressure, binding and transferring poorly soluble drugs in water [9]. A weak drug binding has a short lifetime which is insufficient to provide therapeutic effect, whereas a strong binding reduces the free fraction of drugs with undesirable side effects because of its slow metabolism and excretion [10-13].

Evaluation of mechanisms of interaction of local anaesthetics can provide important information about their storage, transportation, evacuation in the blood makes it possible to predict their pharmacokinetic and pharmacodynamics properties such as the degree and duration of anesthetizing action, the rate of metabolism and/or utilization in peripheral tissues [14-16].
HSA contains a single intrinsic tryptophan residue (Trp 214) in domain IIA and its fluorescence is highly sensitive to the ligands bounded nearby [17-21]. Therefore, it is often used as a probe to investigate the binding properties of drugs with HSA.

Qualitative analysis of chemical binding to HSA can be detected by fluorescence spectra. The excitation wavelength, the emission wavelength, and the fluorescence intensity are the main three parameters used to study the synthetic information of the samples. In addition, the curve spectra can also provide important information. If there is any shift in the excitation or emission wavelength of the spectra, it could be an indication of HSA conformational changes [22].
Fluorescence quenching is formed by either dynamic or static quenching. Dynamic quenching is produced by intermolecular collision between a quencher and fluorescent molecules at an excited state, at which effective collision and the quenching constant should increase with increasing temperature. Usually dynamic quenching does not affect the structure and bioactivity of protein. Static quenching is caused by the intramolecular interaction of quenchers with fluorescent molecules at a ground state, which forms a new complex with changed structures. In static quenching, the constancy of new complexes decreases with the increase in temperature, since high temperatures contribute to molecular diffusion and the detachment of weakly bound complexes. Accordingly, dynamic quenching and static quenching can be distinguished by the impact of temperature change [23].

A considerable amount of scientific research has proven a strong connection between band positions of the IR spectra and changes to the secondary structure of the studied proteins. The energy associated with the observed absorption bands in several proteins are linked to certain molecular vibrations in the secondary structures, such as α helix or β -sheet structures [23-25]. The vital functions of each protein are dependent on the three dimensional structures of its components of peptides and polypeptide.

There are nine IR bands, named amide A, amide B and amides (I -VII), in the order of decreasing frequency [23,24]. Amide I band (1600 -1700) cm^{-1} with its large intensity, is the most useful for the analysis of the secondary structure of proteins. This band involves mainly C=O stretching vibration [26,27]. The amide II band (1480 1600) cm^{-1} and amide III band (1220-1320) cm^{-1} contribute greatly to studies despite of the complex nature of their compositions and can be used for secondary structure prediction [28-30]. The spectra in the region from about (1300-500) cm^{-1} arise due to complicated combinations of (C-C, C-O, C-N) stretching and bending vibration. This range, referred to as the fingerprint region, is important because each compound produces its unique pattern of peaks.

The aim of the present work is to study the interaction between procaine and HSA. The importance of the study comes from the fact that procaine shows a short duration of action and adverse side effects. It is thus highly important for pharmaceutical sciences to clarify the structure, function, and properties of HSA- procaine complexes. Therefore, procaine's storage and transportation by proteins in the blood plasma becomes an important issue which requires investigations of the interaction mechanisms and determining the binding constant between procaine and HSA. In order to attain these objectives, UV-Vis absorption spectroscopy, fluorescence spectroscopy and FTIR spectroscopy were employed to carry out detailed investigation of procaine-HSA association.

Material and Methods

Materials

HSA (fatty acid free) and Procaine hydrochloride in powder form, were purchased from Sigma Aldrich chemical company and were used without any further purifications.

Preparation of stock solutions

HSA was dissolved in phosphate buffered saline (80 mg/ml or 1.2 mM). The concentration of HSA in the buffer solution was calculated using its listed molecular weight of 66.5 kDa. Procaine hydrochloride, with the molecular weight of (272.77 g/mol) [28], was dissolved in double distilled water to prepare the following concentration (0.6, 0.8, 1.0, 1.2, 2.0, 2.4, and 4.80) mM. In the final step, each drug solution was added to an equal volume of the protein solution to attain the desired drug concentrations of (0.3, 0.4, 0.5, 0.6, 1.0, 1.2 and 2.4) mM. The solutions of procaine and HSA were incubated for 2 h at 20°C [31] before any further preparations for spectroscopic measurements.

UV-Vis absorption spectra

The absorption spectra were obtained by the use of a Nano Drop ND-100 spectrophotometer. The absorption spectra were recorded for 5 - 10 µL liquid samples of free HSA (40 mg/ml or

0.6 mM) and for its complexes with procaine solutions with the following concentrations (0.3, 0.4, 0.5, 0.6, 1.0, 1.2, and 2.4) mM. Repeated measurements were taken for all the samples and no significant differences were noticed. The UV-absorption spectra of procaine-HSA complex are obtained at the wavelength of 280 nm.

Fluorescence

The following concentrations of procaine-HSA complex (0.3, 0.4, 0.5, 0.6, 1.0, 1.2, and 2.4) mM were prepared for the fluorescence study. The fluorescence measurements were performed by a Nano Drop ND-3300 Fluorospectrometer at 25°C. The excitation source comes from one of three solid-state light emitting diodes (LED's) with excitation source options include: UV LED with maximum excitation 365 nm, Blue LED with excitation 470 nm, and white LED from 500 to 650 nm excitation. A 2048-element CCD array detector covering 400-750 nm, is connected by an optical fibre to the optical measurement surface. The excitation is performed at the wavelength of 360 nm and the maximum emission wavelength is at 440 nm.

FTIR spectroscopic measurements

The FTIR spectra were measured by a Bruker IFS 66/S spectrophotometer equipped with a liquid nitrogen-cooled MCT detector and a KBr beam splitter. The spectrometer was continuously purged with dry air during the measurements. Samples in the form of thin films are prepared after 2 h of incubation of HSA with procaine solution at room temperature, 30 µl of the complex sample were placed on a certain area on a silicon window plate and left to dry in a closed chamber at room temperature. The dehydrated films were formed on one side of a silicon window with different concentrations of procaine keeping the same protein content in all samples. The obtained absorption spectra were kept in the range of (400-4000) cm^{-1}. Each spectrum was obtained by taking the average of 60 scans to enhance the signal to noise ratio, and the spectral resolution was at 4 cm^{-1}. The aperture setting remained at 8 mm during all measurements, because it gave the best signal to noise ratio.

Baseline correction, normalization and peak areas calculations were done for all the obtained spectra by using OPUS software. The peak positions were determined using the second derivative of the spectra and the use of Fourier self-deconvolution technique. The infrared spectra of HSA and the procaine-HSA comple were recorded for the region of (1200-1700) cm^{-1}. The FTIR spectrum of free HSA was acquired by subtracting the absorption spectrum of the buffer solution from the spectrum of the protein solution. For the net interaction effect, the difference spectra {(HSA-procaine)-(HSA)} were generated using the featureless region of the spectra at (1800-2200 $cm)^{-1}$ as an internal standard [27]. The accuracy of this subtraction method is tested using several control samples with the same protein and drug concentrations, which resulted in a flat base line formation as it should.

The obtained spectral differences were used here, to investigate the nature of the drug-HSA interaction. Silicon windows (NICODOM Ltd) were used as spectroscopic cell windows, 30µl of each sample of HSA-procaine at the following concentrations of (0.15, 0.3, 0.6, 0.7, 0.9) mM was spread on silicon window using spin coater to obtain equal thickness of each sample, and then incubator was used to evaporate the solvent in order to obtain transparent thin film on the silicon window. All solutions were prepared at the same time at room temperature and were stored at the same closed chamber.

Results

UV-Vis absorption spectroscopy

UV-Vis absorption spectroscopy is one of the most common and effective experimental techniques used in calculating binding constants for several drug-protein complexes [32-34]. A complex has formed by the interaction of procaine with HSA as shown from the absorption spectra in **Figure 2**. The intensity of UV absorption of HSA increased with increasing concentrations of procaine indicating formation of procaine-HSA complex. A small red shift of the absorption peak at 280 is noticed with the increase of procaine concentration most likely due to the complex formation of procaine with HSA.

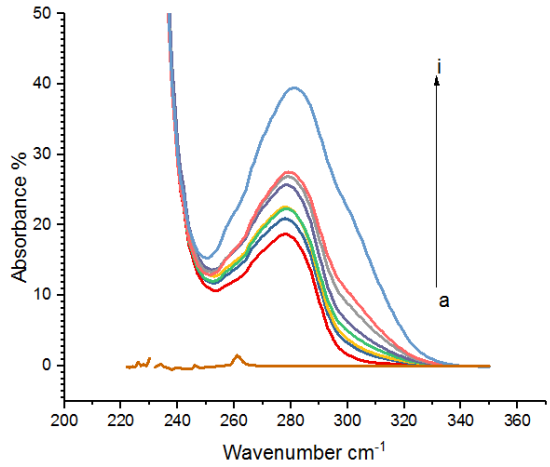

Figure 2: UV-Absorbance spectra of Procaine-HSA complexes at these concentration
(a= Procaine, b= HSA, c=0.3 mM, d=0.4-mM, e=0.5 mM, f=0.6 mM, g=1 mM, h=1.2 mM, i =2.4 mM)

Procaine + HSA ↔ Procaine: HSA (1)

$$K = \frac{[Procaine:HSA]}{[procaine][HSA]} (2)$$

The absorption data were treated using linear reciprocal plots based on the following equation [35].

$$\frac{1}{A - A_0} = \frac{1}{A_\infty - A_0} + \frac{1}{[A_\infty - A_0]K} \cdot \frac{1}{L} (3)$$

Where A_0 corresponds to the initial absorption of protein at 280 nm in the absence of ligand, A_∞ is the final absorption of the ligated protein, and A is the recorded absorption at different procaine concentrations (L). The double reciprocal plot of 1/(A-A_0) versus 1/L is linear (**Figure 3**) and the binding constant (K)

can be calculated from the ratio of the intercept to the slope, which is found to be 1.115 × 103 M^{-1}. This binding constant value shows a relatively weak procaine-HSA interaction in comparison to other drug-HSA complexes with binding constants in the range of 105 and 106 M^{-1} [35-37]. The reason for the weak formation can be attributed to the presence of mainly hydrogen-bonding interaction between protein donor atoms and the procaine polar groups or an indirect drug-protein interaction through water molecules [38].

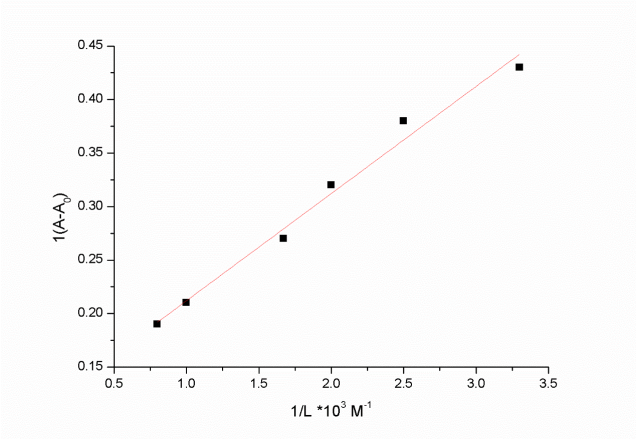

Figure 3: The plot of 1/ (A-A_0) vs. 1/L for HSA with different concentration of procaine

Fluorescence Spectroscopy

Fluorescence quenching refers to any mechanism which reduces the fluorescence intensity of a fluorophore. Fluorescence quenching of HSA results from the tryptophan, tyrosine, and phenylalanine residues. The intrinsic fluorescence of HSA is almost due to the contribution of tryptophan alone, because phenylalanine has very low quantum yield and the fluorescence of tyrosine is almost totally quenched if it is ionized or near an amino group, a carboxyl group, or a tryptophan residue [22]. However, in fluorescence spectra studies on protein- drug interactions, the fluorescence intensity of proteins are usually sensitive to interference by ligands or newly produced complexes which exhibit significant fluorescence at or near the chosen excitation or emission wavelengths [39]. The ligand-binding process during protein-ligand complex is mainly governed by four types of weak, noncovalent forces including hydrogen bond, van der Waals force, electrostatic, and hydrophobic interactions [40].

When HSA is excited at 280 nm, it emits strong intrinsic fluorescence at 440 nm which is shown in **Figure 4**. This phenomenon is due to Trp residue located at the 214th position of the chain and the Try residues in HAS [41,42]. Further, the fluorescence intensity of HSA decreases due to the increase of procaine concentration, while the peak position shows little or no change at all.

The intrinsic fluorescence of HSA is highly sensitive to any slight changes in the local environment of HSA, and becomes obviously weakened by the following factors such as protein conformational transition, bio-molecule binding, and denaturation [43].

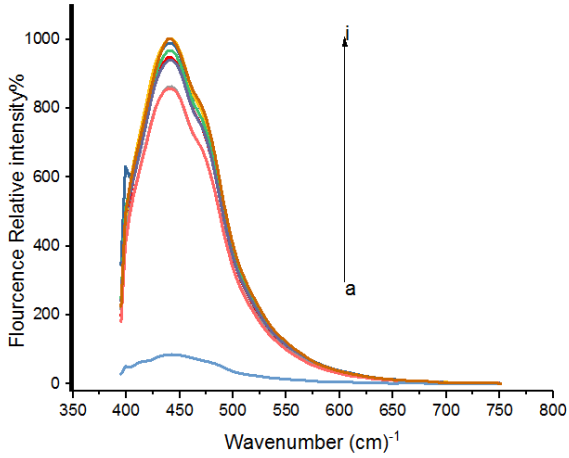

Figure 4: Fluorescence emission spectra of HSA in the presence of various concentration of procaine (a=free procaine 4.8 Mm, b=2.4 mM, c=1.2 mM, d=1.0 mM, e=0.6 mM, f=0.5 mM, g=0.4 mM, h= 0.3 mM, i=free HSA)

The mechanisms of fluorescence quenching are either dynamic quenching or static quenching. Dynamic and static quenching are caused by different means, namely diffusion for dynamic quenching and ground state complex formation for static quenching [38]. In addition, it is known that higher temperatures increase diffusion coefficients leading to an increase in dynamic quenching constants. In contrast, the rise of temperature can decrease the stability of a complex which leads to a decrease in the static quenching constant.

In order to confirm the nature of the quenching mechanism, the fluorescence quenching can be analyzed by the Stern-Volmer equation [44]

$$\frac{F_0}{F} = 1 + K_{q0}[L] = 1 + K_{sv}[L] \quad (4)$$

Where F and F0 are the fluorescence intensities with and without quencher, kq is the quenching rate constant of the biomolecule, Ksv is the Stern Volmer quenching constant, (L) is the concentration of procaine, and τ0 is the average life time of the molecule without quencher 10-8 s.

The value of Ksv (0.00566 × 103 Mol^{-1}) is equal to the slope of a best fit straight-line analysis as shown in **Figure 5**. The quenching rate constant Kq, can be calculated using the fluorescence life time of 10-8 s for HSA [45]. The obtained value for K is 5.66 × 108 Mol^{-1} s^{-1}, which is two orders of magnitude smaller than the maximum scatter collision quenching constant for various quenchers with biopolymer 2×1010 Mol^{-1} s^{-1} [46]. This indicates that procaine has low binding affinity with HSA, and the binding is weak and can be easily reversed. Other low binding constants within similar range of 103 Mol^{-1} have also been reported [47]. Usually, low binding to HSA results in a shorter life time or poorer distribution of drugs in the plasma,

whereas the strong binding reduces the levels of free plasma [48]. Therefore, the binding is weak and can be attributed to combinations of static and dynamic quenching, Lineweaver-Burk equation, is used [49,50]

$$\frac{1}{F_0 - F} = \frac{1}{F_0} + \frac{1}{KLF_0} (5)$$

Where K is the static quenching constant with the unit of L mol^{-1}, which describes the binding efficiency of micro molecules to biological macromolecules at ground state [51]. The value of K can be determined from the slope and the intercept in **Figure 6**. The value of K is 1.156 × 103 Mol^{-1}, which agrees well with the value obtained earlier by UV spectroscopy. The weak quenching constant in this case has led to a lower value of binding constant between the drug and HSA due to an effective hydrogen bonding between procaine and HSA. The interaction of procaine molecules with HSA is initiated by electrostatic forces, but subsequently the hydrophobic interactions play the major role in procaine-HSA interactions. The low value of the binding constant showed that procaine quenched the intrinsic fluorescence of HSA through dynamic quenching mechanism. Furthermore, hydrophobic interaction played a major role in the binding process. Using fluorescence and UV absorption spectroscopy showed that procaine induces protein structural changes. The red shift in **Figure 2**, and the good linearity in the Stern-Volmer equation imply the role of static quenching by procaine [52].

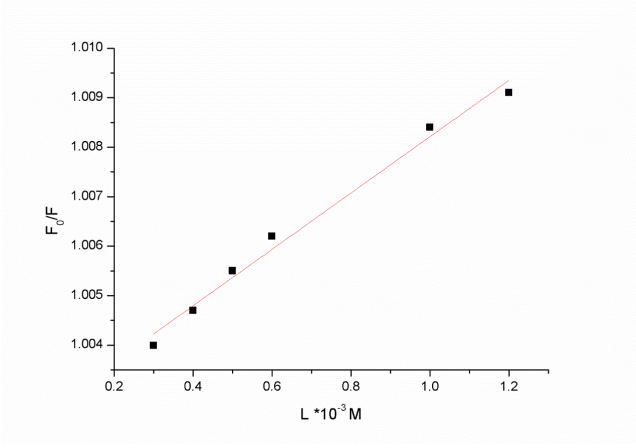

Figure 5: The Stern-Volmer plot for procaine -HSA complexes

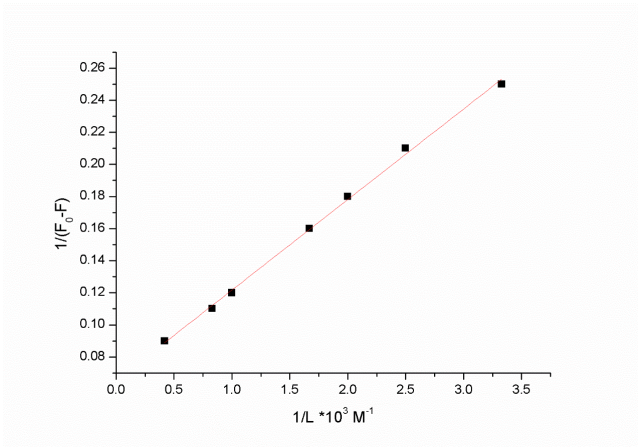

Figure 6: The plot of $1/(F_0 - F)$ vs. 1/[L(10)-3]

FTIR Spectroscopy

The absorption spectra of HSA free and HSA-procaine complex are presented in **Figure 7** showing the major amide bands (I, II, III) and the fingerprint region. All major peaks have been identified by taking the second derivative of the spectra and by applying Fourier self-deconvolutions (FSD) to the spectra as shown in **Figure 8**.

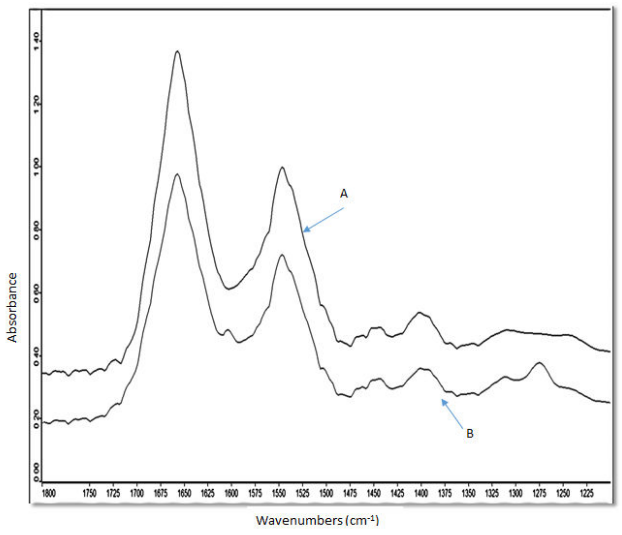

Figure 7: Spectra of HSA free (A) and Procaine-HSA complex 0.9 mM (B)

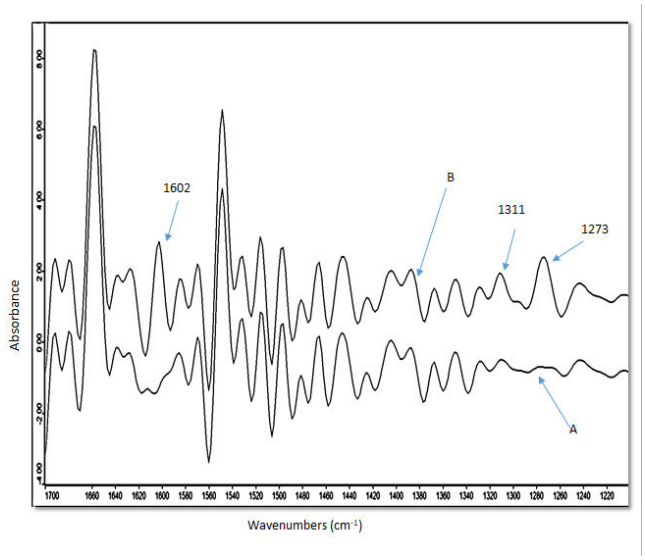

Figure 8: FSD Spectra of (A) HSA free and (B) HSA-Procaine complex 0.6 mM

The peak positions for the spectra of the protein and its complex with procaine are listed in **Table 1**. Infrared spectra of proteins exhibit a number of amide bands, which represent different vibrations of the peptide moiety. The FSD analysis of the absorption spectra for HSA in the amide I region (1600 -1700) cm^{-1} reveals the separate components of the band. The peaks of these bands correspond to the C-O stretching vibrations of the amide I group, coupled to the C-N stretching and C-C-N deformation mode [51]. The individual components of amide II (1600-1480) cm^{-1} are mainly due to out of phase combination of N- H in-plane bending and C-N stretching vibration modes [53]. As for amide III (1220=1320) cm^{-1}, the absorption bands are caused by in-phase combination of the N-H bending and the C-N stretching vibration with some contributions from the C-O in-plane bending and the C-C stretching vibration [53,54].

The component bands of amide I were attributed according to the well-established assignment criterion [55,56]. The bands range (1615-1637) cm^{-1} and (1680-1700) cm^{-1} are generally assigned to β-sheets, (1638-1648) cm^{-1} are assigned to random coil, (1649 -1660) cm^{-1} to α -helix and (1660-1680) cm^{-1} to β-turn structure. The amide II components are assigned in the following order (1488-1504) and (1585-1600) cm^{-1} to β=sheets, (1504-1527) cm^{-1} to random coil, (1527 -1560) cm^{-1} to α- helix and (1564-1585) cm^{-1} to turn structure [57]. The component bands of Amide III have been assigned as follows: α-helix (1330-1290) cm^{-1}, β-turn (1290-1270) cm^{-1}, random coil (1270-1250) cm^{-1} and β-sheets (1250-1220) cm^{-1}[56].

The peak positions of amide I bands in HSA spectrum stayed about the same as shown in **Table 1**. The only noticeable change is the disappearance of the small peak at 1612 cm^{-1} and the rise of a new peak at 1602 cm^{-1} with higher concentration of procaine. The amide II bands did not show any major changes in their peak positions with the different concentrations of HSA-Procaine complexes. As for amide III, the following peaks (1310, 1294, 1243, and 1224) cm^{-1} maintain their positions, while the two weak bands at 1277 and 1243 cm^{-1} have been over shadowed by a new peak at 1273 cm^{-1}. The two new peaks at 1602 and 1273 cm^{-1} are due to C=C (aromatic) stretching mode and C-O and C-N stretching mode of procaine, respectively [58-60]. Their dominant effect appears to be due to the presence of unbound procaine molecules within the HSA-procaine complex which is related to the weak binding constant between procaine and HSA.

Table 1: Absorption peak positions in Wave numbers (cm^{-1}) for Procaine-HSA at different concentrations.

Bands	Range (cm^{-1})	Free HSA	concentrations				
Amide I	1700-1600	0	0.15 mM	0.3 mM	0.6 mM	0.7 mM	0.9 mM
B-sheets		----	-----	1603	1603	1603	1603
		1613	1612	--	--	--	--
	β-sheets	1627	1628	1626	1626	1626	1627
	Random	1640	1641	1640	1640	1641	1641
	α-helix	1657	1658	1658	1657	1659	1659
	Turns	1679	1678	1678	1679	1679	1679
	β-sheets	1694	1694	1694	1694	1694	1694
Amide II	$1600^{-1}480$						
	β-sheets	1498	1498	1498	1498	1498	1498
	β-sheets	1515	1516	1515	1515	1516	1516
	Random	1532	1532	1532	1532	1532	1532
	α-helix	1549	1549	1549	1549	1549	1549

	Turn	1569	1569	1569	1569	1569	1569
	β-sheets	1585	1585	1585	1584	1584	1584
Amide III	1320-1220						
	β-sheets	1224	1224	1224	1224	1224	1224
	β-sheets	1244	1244	1244	1244	1244	1244
	Random	1267	1267				
				1273	1273	1273	1273
	Random	1277	1277				
	Turns	1295	1295	1295	1295	1295	1295
	α-helix	1309	1309	1309	1310	1310	1310

The relative intensities of all component bands of amide I, amide II, and amide III were calculated and listed in **Table 2**. The following bands showed major increase in their intensities with increasing procaine concentration in the complex (1603, 1309, and 1273) cm^{-1}, while these bands (1627, 1548) cm^{-1} showed very small increase in their relative intensities. On the other hand, the following bands (1657, 1531, and 1294) cm^{-1} show little or no decrease in their intensities. The bands at (1613, 1277, and 1266) cm^{-1} disappeared due to overlapping by neighboring bands and the rest of the bands showed no change in their intensities.

Table 2: Relative intensity of absorption bands for Procaine-HSA at different concentrations.

Bands	**Range (cm^{-1})**	**Intensity %**	**Intensity %**	**Intensity %**	**Intensity %**	**Intensity %**	**Intensity %**
Amide I	$1700^{-1}600$	0	0.15 mM	0.3mM	0.6mM	0.7mM	0.9mM
β-sheets	1606-1620	3	5				
β-sheets	1620-1633	5	7	7	9	17	14
Random	1633-1647	8	8	9	9	10	8
α-helix	1649-1670	46	40	40	46	25	39
Turns	1672-1686	18	19	20	18	21	18
β-sheets	1687-1700	20	21	24	18	26	21
Amide II	1600-1480						
β-sheets	1487 1506	12	12	13	13	14	14
β-sheets	1506-1523	14	13	13	14	11	13
Random	1523-1539	11	15	11	10	10	9
α-helix	1541- 1558	23	25	23	25	20	24
Turns	1560-1585	19	19	19	20	21	21
β-sheets	1585-1600	21	16	21	18	24	19
Amide III	1320-1220						
β-sheets	1222-1256	51	41	42	34	30	29

Random	1259-1287	15	21	30	40	43	45
Turns	1288-1302	5	6	5	5	5	5
α-helix	1302-1319	29	32	23	21	22	21

The difference in FSD spectra [(HSA+ procaine)-(HSA)] were obtained to investigate the intensity variations and the results are shown in **Figure 9**. The strong negative features at 1601 and 1277 cm^{-1} were due to absorbance by free procaine. While the band at 1309 cm^{-1} formed by double contributions from free procaine and procaine-HSA complex. The positive peaks shown at 1657 and 1554 cm^{-1} represent the decrease in intensity of the α-helix bands of the amide I and amide II respectively. This decrease is attributed to the unfolding of the protein in the presence of procaine as a result of the H-bonding formation with protein C=O and C-N groups [61]. As for any possible changes in the intensity of α-helix in the amide III region, it could not be determined due to the overlapping by the procaine band at 1309 cm^{-1}. In general these changes of the peak positions, intensities and peak shapes are considered to be overwhelming evidences of secondary structure changes have occurred as a result of procaine interaction with HSA.

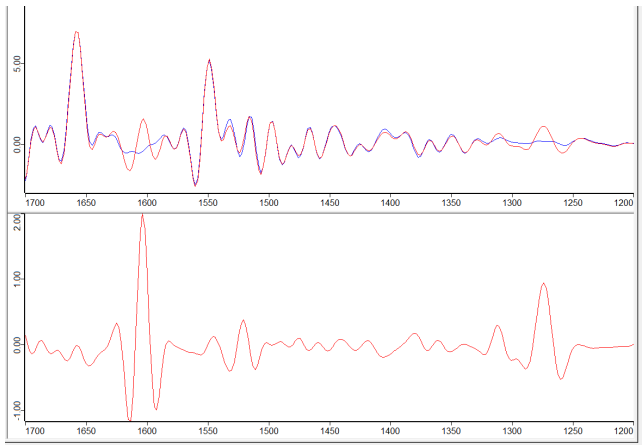

Figure 9: Top Part shows HSA spectra (B) and HSA-procaine 0.6 mM (A). Bottom part shows the difference Spectra between (HSA-procaine complex) - (free HSA).

Conclusions

In this paper, the interaction between procaine and HSA was investigated by fluorescence spectroscopy, UV-Vis absorption and FTIR spectroscopy. The results indicate that the fluorescence quenching mechanism of HSA by Procaine binding indicate contributions from both a static and dynamic quenching process. The binding reaction of procaine with HSA showed a binding constant is in the range of (1.115-1.156) × 103 M^{-1}. The experimental results pointed to contributions from different interaction mechanisms between procaine and HSA. It seems that, the complexation of procaine molecules with HSA is initiated by electrostatic forces, but subsequently the hydrophobic interaction played a major role in this complexation.

The infrared spectroscopic results show that drug- protein binding occurs with the participation of the tryptophan residues and some conformation of the protein secondary structure. The variations in the relative intensities of the absorption bands showed a slight decrease in α-helical contents and a minor increase in β-sheet contents.

References

1. Hosseinzadeh R, Gheshlagi M, Tahmasebi R, Hojjati F (2009) spectrophotometric study of interaction and solubilization of procaine hydrochloride in micellar systems. Cent Eur J Chem 7: 90-95
2. Lazdunski C, Baty D (1979) Procaine, a local anesthetic interacting with the cell membrane, inhibits the processing of precursor forms of periplasmic proteins in Escherichia coli. Eur J Biochem 96: 49-57
3. Sawaki K, Kawaguchim M (1984) Some Correlations between procaine-induced convulsions and monoamides in the spinal cord of rats. Jpn J Pharmacol 51: 369-376
4. Madrakian T, Bagheri H, Afkhami A, Soleimani M (2014) Spectroscopic and molecular docking techniques study of the interaction between oxymetholone and human serum albumin. J lumin 155: 218-225
5. Carter DC, He XM, Munson SH, Twigg PD, Gernert KM, et al. (1994) Three-dimensional Structure of Human Serum Albumin. Science 244: 1195-1198
6. He XM, Carter DC (1998) Atomic structure and chemistry of human serum albumin. Nature 358: 209-215
7. Yang F, Zhang Y, Liang H (2014) Interactive Association of Drugs Binding to Human Serum Albumin. Int J Mol Sci 15: 3580-3595
8. Kragh-Hansen U (1981) Molecular aspects of ligand binding to serum albumin. Pharmacol Rev 33: 17
9. T. Peters (1985) Serum albumin. Adv Protein Chem 37: 161
10. Zhang YZ, Zhou B, Liu YX, Zhou CX, Ding XL et al. (2008) Fluorescence study on the interaction of bovine serum albumin with p-aminoazobenzene. J Fluoresc 18: 109-118
11. Kragh-Hansen U (1990) Structure and ligand binding properties of human serum albumin. Dan Med Bull 37: 57-84
12. Cheger SI (1975) Transport Function of Serum Albumin, The academy of sciences, Bucharest,178
13. Sudlow G, Birkett DJ, Wade DN (1975) The characterization of two specific drug binding sites on human serum albumin. Mol Pharmacol 11:824-832
14. Haque SJ, Poddar MK (1984) Interactions of cannabinoids with bovine serum albumin. Biosci Rep 4: 239-243

15. Purohit G, Sakthivel T, Florence AT (2003) The interaction of cationic dendrons with albumin and their diffusion through cellulose membranes. Int J Pharm 254: 37-41

16. Mazoit JX, Cao LS, Samii K (1996) Binding of bupivacaine to human serum proteins, isolated albumin and isolated alpha-1-acid glycoprotein. Differences between the two enantiomers are partly due to cooperativity. J Pharmacol Exp Ther 276: 109-115

17. S.S. Krishnakumar, D. Panda (2002) Spatial Relationship between the Prodan Site, Trp-214, and Cys-34 Residues in Human Serum Albumin and Loss of Structure through Incremental Unfolding. Biochemistry 41: 7443

18. Il'ichev YV, Perry JL, Simon JD (2002) Interaction of Ochratoxin A with Human Serum Albumin. Preferential Binding of the Dianion and pH Effects J Phys Chem B 106: 460

19. Yasseen Z J, Ghossain ME (2016) Studies on Binding of Widely used Drugs with Human Serum Albumin at Different Temperatures and PHs. J Biomedical Sci 5:3

20. Alanazi AM, Abdelhameed AS (2016) A spectroscopic approach to investigate the molecular interactions between the newly approved irreversible ErbB blocker "Afatinib" and bovine serum albumin. PLoS ONE, e0146297

21. Darwish SM,Sharkh SEA,Teir MMA,Makharza SA,Abu-hadid MA (2010) Spectroscopic investigations of pentobarbital interaction with human serum albumin. J Mol Struct 963: 122-129

22. Guowen Z, Qingmin Q, Junhui P, Jinbao G (2018) Study of the interaction between icariin and human serum albumin by fluorescence spectroscopy. Journal of Molecular Structure 881: 132-138

23. Elliot A, Ambrose EJ (1950) Structure of Synthetic Polypeptides. Nature 165: 921-922

24. Miyazawa T (1967) in Poly-a-amino Acids, ed. Fasman, G.D.(Marcel Dekker, Inc., NewYork), 69-103

25. Krimm S, Bandekar J (1986) Vibrational spectroscopy and conformation of peptides, polypeptides, and proteins. Adv Protein Chem 38: 181-364

26. Byler DM, Susi H (1986) Examination of the secondary structure of proteins by deconvolved FTIR spectra. Biopolymer, 25: 469–487

27. Surewicz WK, Mantsch HH, Chapman D (1993) Determination of Protein Secondary Structure by Fourier Transform Infrared Spectroscopy: A Critical Assessment. Biochemistry 3: 389-394

28. Xie MX, Liu Y, Studies on amide III infrared bands for the secondary structure determination of proteins. Chem J Chin Univ-Chinese 24: 226-231

29. Cai S, Singh BR (1999) Identification of ß-turn and random coil amide III infrared bands for secondary structure estimation of proteins. Biophys Chem 80: 7-20

30. Cai S, Singh BR, (2004) A distinct utility of the amide III infrared band for secondary structure estimation of aqueous protein solutions using partial least squares methods. Biochemistry 43:2541-2549

31. Galenko-Yaroshevskii P, Fistunenko PN, Dukhanin AS (2005) Kinetics of Interaction of Local Anesthetics with Human Serum Albumin. Bull Exp Biol Med 140

32. J.J. Stephanos (1996) Drug-protein interactions: two-site binding of heterocyclic ligands to a monomeric hemoglobin. J Inorg Biochem 62: 155

33. I.M. Klotz, (1982) Numbers of receptor sites from Scatchard graphs: facts and fantasies. Science 217: 1247-1249

34. Zhong W, Wang Y, Yu JS, Liang Y, Ni K, et al. (2004) The interaction of human serum albumin with a novel antidiabetic agent--SU-118. J Pharm Sci 93: 1039

35. Stephanos J, Farina S, Addison A (1996) Biochem. Biophys. Acta 1295: 209

36. Colmenarejo G, Alvarez-Pedraglio A, Lavandera JL (2001) Cheminformatic Models To Predict Binding Affinities to Human Serum Albumin. J Med Chem 44: 4370-4378

37. Valko K, Nunhuck S, Bevan C, Abraham MH, Reynold DP (2003) Fast Gradient HPLC Method to Determine Compounds Binding to Human Serum Albumin. Relationships with Octanol/Water and Immobilized Artificial Membrane Lipophilicity 92

38. Purcell M, Neault JF, Tajmir-Riahi HA (2000) Biochim Biophys Acta 1478: 61

39. Xie LX, Wu LH, Kang C, Xiang SX, Yin XL, Gu HW et al. (2015) Quantitative Investigation of the Dynamic Interaction of Human Serum Albumin with Procaine Using a Multi-way Calibration. Anal Methods 7: 6552

40. Maiti TK, Ghosh KS, Debnath J, Dasgupta S (2006) Binding of all-trans retinoic acid to human serum albumin: fluorescence, FT-IR and circular dichroism studies. Int J Biol Macromol 38: 197-202

41. Shahrakia S, Shiria F, Mansouri-Torshizib H (2016) Biophysical and Molecular Docking Studies of Human Serum Albumin Interactions with a Potential Anticancer Pt(II) Complex. Biomacromol J 2: 65-77

42. Ranjbar S, Shokoohinia Y, Ghobadi S, Bijari N, Gholamzadeh S, et al.(2013) Studies of the Interaction between Isoimperatorin and Human Serum Albumin by Multi spectroscopic Method: Identification of Possible Binding Site of the Compound Using Esterase Activity of the Protein. Scientific World Journal 1-13

43. Nanda RK, Sarkar N, Banerjee R (2007) Probing the interaction of ellagic acid with human serum albumin: a fluorescence spectroscopic study. J Photochem Photobiol A Chem 192: 152-158

44. Tian JN, Liu JQ, Zhang JY, Hu ZD, Chen XG (2003) Fluorescence Studies on the Interactions of Barbaloin with Bovine Serum Albumin. Chem Pharm Bull 51: 579

45. Chen GZ, Huang XZ, Xu JG, Zheng ZZ, Wang ZB (1990) Method of Fluorescence Analysis, Science Press, Beijing, ch 4

46. Vaughan WM, Weber G (1970) Oxygen quenching of pyrenebutyric acid fluorescence in water: a dynamic probe of the microenvironment. Biochemistry 9:464-473

47. Cheng TG, Li QL, Zhou ZG, Wang YL, Bryant SH (2012) Structure-Based Virtual Screening for Drug Discovery: A Problem-Centric Review. AAPS J 14: 133-141

48. Chen YC, Wang HM, Niu QX, Ye DY, Liang GW (2016) Binding between Saikosaponin C and Human Serum Albumin by Fluorescence Spectroscopy and Molecular Docking. Molecules 21: 153

49. Yan CN, Zhang HX, Liu Y, Mei P, Li KH, Tong JQ (2005) Fluorescence spectra of the binding reaction between paraquat and bovine serum albumin. Actachim. Sinica 63: 1727-1732

50. Yan CN, Zhang HX, Liu Y, Mei P (2005) Study on binding reaction between flucytosine and bovine serum albumin. Chin J chem 23: 1151-1156

51. Dukor RK, Chalmers JM, Griffiths PR (2001) Vibrational Spectroscopy in the Detection of Cancer, Handbook of Vibrational Spectroscopy, 5: Ch 3

52. Chen YC, Wang HM, Niu OX, Ye DY, Liang GW (2016) Binding between Saikosaponin C and Human Serum Albumin by Fluorescence Spectroscopy and Molecular Docking, Molecules 21: 153

53. Sirotkin VA, Zinatullin AN, Solomonov BN, Faizullin DA, Fedotov VD (2001) Calorimetric and Fourier transform Infrared Spectroscopic Study of Solid Proteins Immersed in Low Water Organic Solvents. Biochimicae Biophysica Acta, 1547: 359-369.

54. Chirgadze YN, Fedorov OV, Trushina NP (1975) Secondary structure of Na+, K+-dependent adenosine triphosphatase. Biopolymers 14: 679-694

55. Byler DM, Brouilette JN, Susi H (1986) Examination of the secondary structure of proteins by deconvolved FTIR spectra. Spectroscopy 1: 39

56. Neault JF, Tajmir-Riahi HA (1998) Interaction of cisplatin with human serum albumin. Drug binding mode and protein secondary structure, Biochimica et Biophysica Acta 1384: 153-159

57. Ivanov A I, Zhbankov R G, Korolenko E A, Korolik E V, Meleshchenko L A, Marchewka M, H. et al. 1994, J. Appl. Spectrosc. 60: 305-309

58. Merine H, Tennouga L, Mesli A, Chafi N, Medjahed K (2013) Kinetic Study of the Controlled Release of Procaine Grafted in Monomer and Copolymer Supports in both Homogeneous and Heterogeneous Medium, AJPST 3: 99-106

59. Brittain HG (1990) Analytical profiles of drug substances and excipients Academic press. 26 ISBN:0-12-260826-7

60. Fuliaş A, Ledeţi I, Vlase G, Popoiu C, Hegheş A, et al. (2013) Thermal behavior of procaine and benzocaine Part II: compatibility study with some pharmaceutical excipients used in solid dosage forms. Chem Cent J 7: 7-140

61. Darwish SM (2010) Spectroscopic study of propofol binding to human serum albumin. Biophys Rev Lett 5: 209-226